pared to $Mn_2Mn(hfac)_6(NITpPy)_2$. The saturation magnetization in this case corresponds to $S = 5$. This value and the absence of any evidence of spin flipping in an external magnetic field agree with the structural model we have obtained. In fact the expected antiferromagnetic interaction between the radical and nickel(II) through the pyridine nitrogen[9] leads to a parallel arrangement of nickel and manganese spins and to $S = 5$ for the formula unit. The magnetic phase transition occurs at higher temperature in III than in I in agreement with the larger magnetic moment of III compared to I.

Within this assumption the high-temperature susceptibility must be given by the sum of that of the manganese–radical chains of the side-pieces plus the contribution of an uncoupled nickel(II) ion. In fact χT could be fitted to give $J = 367$ (3) cm^{-1}. The difference between the J values estimated from the data of I and III is probably related to the different contribution of the off-chain metal ions which in I tends to reduce the susceptibility and in II tends to increase it.

The interpretation of the data for $Mn_2Co(hfac)_6(NITpPy)_2$ is complicated by the anticipated large anisotropy associated with the octahedral cobalt(II),[28] which is bound to unquenched orbital contributions. This anisotropy may be responsible for the different behavior of the ac susceptibility of II compared to I and III; however also in this case, the lack of metamagnetic behavior suggests that the off-chains sites are essentially occupied by cobalt(II) ions.

(28) Banci, L.; Bencini, A.; Benelli, C.; Gatteschi, D.; Zanchini, C. *Struct. Bonding (Berlin)* **1982**, *52*, 32.

Conclusions

The analysis of the magnetic properties of $Mn_2M(hfac)_6(NITpPy)_2$ allowed us to suggest a structure for these compounds. We think we have provided sound evidence that in these materials, chains $Mn(hfac)_2(NITpPy)$ are connected by $M(py)_2$ groups. These compounds therefore provide examples of low dimensional materials in which three different spins regularly alternate in space. A possible description is that of regular bimetallic ribbons (or layers) in which the metal ions are bridged by tridentate NITpPy radicals. Our original goal was that of increasing the critical temperatures to three-dimensional order by cross-linking the $Mn(hfac)_2(NITR)$ chains. Although we have succeeded to some extent in connecting the chains, the critical temperatures have not increased.

Acknowledgment. Thanks are due to Professor A. C. Fabretti, University of Modena, for recording the IR spectra. The financial contributions of MURST and of Progetto Finalizzato Materiali Speciali per Technologie Avanzate are gratefully acknowledged.

Registry No. I, 137845-54-6; II, 137845-56-8; III, 137845-58-0.

Supplementary Material Available: Figure S1 and Figure S2 showing the temperature dependence of the magnetic susceptibility for $Mn_2Co(hfac)_6(NITpPy)_2$ and $Mn_2Ni(hfac)_6(NITpPy)_2$, respectively, and, in the inset of Figure S2, the calculated susceptibility. (2 pages). Ordering information is given on any current masthead page.

Electrochemical Quartz Crystal Microbalance Monitoring of Cadmium Sulfide Generation in Polypyrrole and Polypyrrole Poly(styrenesulfonate) Thin Films

Maria Hepel,*[,1] Edith Seymour,[1] David Yogev,[2] and Janos H. Fendler*[,2]

Department of Chemistry, State University of New York at Potsdam, Potsdam, New York 13676, and Department of Chemistry, Syracuse University, Syracuse, New York 13244-4100

Received August 12, 1991. Revised Manuscript Received November 4, 1991

Cadmium sulfide, CdS, particles have been in situ generated electrochemically in polypyrrole, PPy, and polypyrrole–poly(styrenesulfonate), PPy/PSS^-, composite thin films on a gold-coated quartz crystal electrode. Two different approaches have been taken. In the first approach, cadmium ions have been attached to the PPy/PSS^- composite thin film, formed upon subjecting an aqueous deoxygenated 2.0×10^{-2} M pyrrole solution to an $E = 0$ to $E = 600$ mV potential step in the presence of 1.0×10^{-3} M PSS^- and 0.10 M NaCl. Addition of cadmium ions followed by the introduction of bisulfide ions (HS^-) has led to the formation of CdS particles at a number of nucleation sites. In the second approach, HS^- ions have been electrochemically oxidized to elementary sulfur in the matrices of PPy thin films, formed upon applying a potential step from $E = 0$ to $E = 650$ mV to an aqueous deoxygenated 2.0×10^{-2} M pyrrole solution in the presence of a 0.10 M NaCl supporting electrolyte. Subsequent to the removal of excess HS^- (by ion exchange by Cl^-) cadmium ions have been added to the solution bathing the PPy-coated electrode. Cathodization has then reduced both the oxidized form of PPy and the elementary sulfur and has led to the formation of CdS particles at a large number of nucleation sites. Interfacial mass changes which have accompanied the formation of PPy and PPy/PSS^- thin films and CdS formation therein have been monitored by an electrochemical quartz crystal microbalance. Scanning electron microscopy and X-ray diffraction measurements have confirmed the presence of nonuniform CdS particles in the PPy and PPy/PSS^- films.

Introduction

Beneficial mechanical, optical, electrical, electrooptical, electrochemical, and chemical properties render conducting polymer–semiconductor heterojunctions to be useful in a number of applications, including solar energy conversion.[3-5] On the one hand, surface coating by polypyrrole

(1) State University of New York at Potsdam.
(2) Syracuse University.

(3) *Energy Resources through Photochemistry and Catalysis*; Grätzel, M., Ed.; Academic: New York, 1983.
(4) *Organic Phototransformations in Nonhomogeneous Media*; Fox, M. A., Ed.; American Chemical Society: Washington, DC, 1985.

0897-4756/92/2804-0209$03.00/0

(PPy) has been shown to stabilize cadmium sulfide against photodegradation.[6,7] On the other hand, inorganic and organic molecules, dyes, drugs, and semiconductors have been incorporated into PPy and related conducting polymers[8-15] and have been used as sensors and electronic and controllable release devices.

PPy can be synthesized by the electrochemical oxidation of monomeric pyrrole in aqueous electrolyte solutions.[16] Electrochemically generated PPy is partially oxidized. Polarons and bipolarons (i.e., cation and dication radicals associated with lattice distortions) have been postulated to be responsible for the observed conductivity in PPy films.[17] Anions (Cl^-, ClO_4^-, and BF_4^-, for example) play an important role in the electropolymerization of pyrrole and in the subsequent behavior of the PPy film formed. Particularly significant is the formation of PPy/poly(styrenesulfonate) composites (PPy/PSS^-) by the electrochemical polymerization of pyrrole in the presence of sodium poly(styrenesulfonate) (PSS^-Na^+).[18-24] Depending on their size and binding constants, ions can be inserted or removed during and subsequent to the electrochemical growth of the PPy film.[18] PPy films have predominant anionic dynamics (i.e., they incorporate and release anions) and composite PPy/PSS^- films have predominant cationic dynamics (i.e., they incorporate and release cations) during redox reactions of the polymer. These principles have been utilized in the present work for the in situ generation of cadmium sulfide (CdS) particles in polymer films.

Two different approaches have been taken in forming CdS particles in PPy films. In the first approach (method I), cadmium ions were incorporated into PPy/PSS^- films. Addition of bisulfide ions (HS^-) led to the formation of CdS particles at a number of nucleation sites. In the second approach (method II), HS^- ions introduced into the PPy film were immobilized by electrochemical oxidation to elementary sulfur. Subsequent to the removal of excess HS^- (by ion exchange by Cl^-) cadmium ions were added to the solution bathing the PPy-coated electrode. Cathodization then reduced both the oxidized form of PPy and the elementary sulfur and led to the formation of CdS particles at a large number of nucleation sites.

The success of the two methods used for the in situ CdS formation depended on our ability to select the best conditions for the introduction of the desired precursors into the PPy matrix. By applying an electrochemical quartz crystal microbalance (EQCM),[11-12,25-31] we have been able to monitor the interfacial mass changes which accompanied PPy film formation, introduction of CdS precursors into the PPy film, and CdS particle formation in the PPy film. The EQCM technique is based on the piezoelectric effect. Deposition (or removal) of nanogram quantities of material decreases (or increases) the oscillating frequency of the quartz crystal vibration by measurable amounts. For thin rigid films, interfacial mass changes (Δm) are related to changes in EQCM oscillation frequency (Δf) by the Sauerbrey equation:[30]

$$\Delta f = -2\Delta m n f_0^2 / A\sqrt{\mu_q d_q} \quad (1)$$

where d_q is the density ($d_q = 2.6848$ g/cm^3) and μ_q is the shear modulus ($\mu_q = 2.947 \times 10^{11}$ g/cm) of the quartz crystal, A is the piezoelectrically active area (in cm^2), f_0 is the resonance frequency of the unloaded quartz crystal, and n is the overtone number.

In situ formation of CdS particles in the PPy films have been confirmed by scanning electron microscopic and X-ray diffraction measurements.

Experimental Section

Materials. Pyrrole (Merck Co.) was vacuum distilled and stored in a dark bottle in the refrigerator. Sodium poly(styrenesulfonate) (PSS^-Na^+), reagent-grade sodium chloride, potassium chloride, cadmium chloride (Fisher Scientific), and sodium sulfide (Baker Chemical Co.) were used as received. Solutions were prepared in Millipore Milli-Q deionized water and deoxygenated by bubbling by purified nitrogen (Matheson). A 10-MHz AT-cut quartz crystal of approximately 12-mm diameter with vacuum-deposited gold (ca. 900 Å thick) on both sides (International Crystal Manufacturing Co., Oklahoma City, OK) was used as a substrate for polymer deposition and CdS generation therein.

Measurements. The gold-coated quartz crystal substrate constituted the bottom of a 100-mL glass EQCM cell. It was sealed to the cell by silicone rubber cement (General Electric). In the exterior of the cell, the substrate was connected to the oscillator and in the interior it functioned as the working electrode with an active area of 0.50 cm^2. The working electrode was polarized by using a platinum wire counter electrode. The potential of the counter electrode was measured against and quoted with respect to a KCl-saturated calomel reference electrode (SCE). A Model RDE4 potentiostat-galvanostat (Pine Instrument Company) was used to control and to measure the electrochemical events. The resonant frequency of the quartz crystal during the electrochemically induced mass changes was monitored using a home-built oscillator circuit. The frequency was measured using a Model HP 1255 frequency counter (Hewlett-Packard). A Hewlett-Packard Model 7090 data acquisition system was used for the simultaneous recording of current vs. potential and quartz crystal oscillation frequency vs potential, or current vs time and frequency vs time. Since the oscillation frequency decrease corresponds to

(5) Fendler, J. H. *J. Phys. Chem.* **1985**, *89*, 2730.
(6) Frank, A. J.; Cooper, J.; Noufi, R.; Turner, J. A.; Nozik, A. J. In *Photoelectrochemistry: Fundamental Processes and Measurement Techniques*; Wallace, W. L., Nozik, A. J., Deb, S. J., Wilson, R. H., Eds.; The Electrochemical Society: Princeton, 1982; p 248.
(7) Honda, K.; Frank, A. J. *J. Phys. Chem.* **1984**, *88*, 5577. Frank, A. J.; Honda, K. *J. Electroanal. Chem.* **1983**, *150*, 673.
(8) Pernaut, J. M.; Peres, R. C. D.; Juliano, V. F.; De Padi, M.-A. *J. Electroanal. Chem.* **1989**, *274*, 225.
(9) Yoneyama, H.; Shoji, Y. *J. Electrochem. Soc.* **1990**, *137*, 3826.
(10) Zhou, A. X.; Miller, L. L.; Valentine, J. R. *J. Electroanal. Chem.* **1989**, *261*, 147.
(11) Hepel, M. *Proc. Int. Symp. on Composites*; Orlando, FL, Nov. 12-15, 1990. In *Ceramic Transactions*, Advanced Composites Materials; Sacks, M. D., Ed.; American Chemical Society: Washington, DC, 1991; Vol. 19, pp 385-396.
(12) Hepel, M. *Proc. 3rd Int. Meeting on Chemical Sensors*; Cleveland, OH, Sept 24-26, 1990; pp 35-37.
(13) Hepel, M.; Janusz, W. *Abstr. Proc. 64th Colloid Surf. Sci. Symp.* **1990**, 159.
(14) Bull, R. H.; Fan, F. R. F.; Bond, A. J. *J. Electrochem. Soc.* **1984**, *131*, 687.
(15) Dalas, E.; Sakkopoulos, S.; Kallitsis, J.; Vitoratos, E.; Koutsoukos, P. G. *Langmuir* **1991**, *6*, 1356.
(16) Seymour, R. V. *Conducting Polymers*; Plenum Press: New York, 1981. Skotheim, T. A. *Handbook of Conducting Polymers*; Marcel Dekker: New York, 1986.
(17) Bredas, J. L.; Street, G. B. *Acc. Chem. Res.* **1985**, *18*, 309.
(18) Naoi, K.; Lien, M.; Smyrl, W. H. *J. Electrochem. Soc.* **1991**, *138*, 440.
(19) (a) Shimidzu, T.; Ohtani, A.; Iyoda, T.; Honda, K. *J. Electroanal. Chem.* **1987**, *224*, 123. (b) Shimidzu, T.; Ohtani, A.; Honda, K. *J. Electroanal. Chem.* **1988**, *251*, 323.
(20) Bidan, G.; Ehui, B.; Lapkowski, M. *J. Phys. D., Appl. Phys.* **1988**, *21*, 1043.
(21) Noftle, R. E.; Pletcher, D. *J. Electroanal. Chem.* **1987**, *227*, 229.
(22) Warren, L. F.; Anderson, D. A. *J. Electrochem. Soc.* **1987**, *134*, 101.
(23) Glatzhofer, D. T.; Ulanski, J.; Wegner, G. *Polymer* **1987**, *28*, 449.
(24) Baker, C. K.; Qiu, Y.-J.; Reynolds, J. R. *J. Phys. Chem.* **1991**, *95*, 4446.
(25) Kanazawa, K. K.; Gordon, J. G. *Anal. Chim. Acta* **1985**, *175*, 99.
(26) Bruckenstein, S.; Wilde, C. P.; Hillman, A. R. *J. Phys. Chem.* **1990**, *94*, 6458.
(27) Hillman, A. R.; Loveday, D. C.; Bruckenstein, S. *J. Electroanal. Chem.*, in press.
(28) Orata, D.; Buttry, D. A. *J. Am. Chem. Soc.* **1987**, *109*, 3574.
(29) Ward, M. D. *J. Phys. Chem.* **1988**, *92*, 2049.
(30) Sauerbrey, G. *Z. Phys.* **1959**, *155*, 206.
(31) Diaz, A. F.; Kanazawa, K. K.; Gorrolini, G. P. *J. Chem. Soc., Chem. Commun.* **1979**, 635.

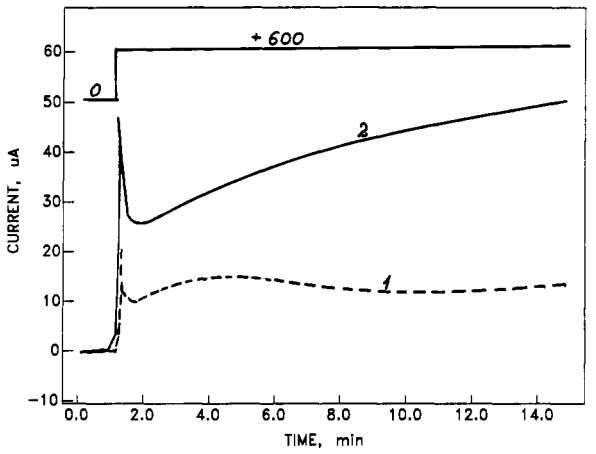

Figure 1. Current–time transients obtained at gold modified EQCM electrodes during the polymerization process of an aqueous deoxygenated 2.0×10^{-2} M pyrrole solution containing 0.1 M NaCl in the absence of PSS^- at a potential step of $E = 0$ to $E = 650$ mV (vs SCE; 1) and in the presence of 1.0×10^{-3} M PSS^- at a potential step of $E = 0$ to $E = 600$ mV (2).

the mass increase and only the latter is the subject of interpretation, we assume a convention of plotting frequency decreases upward and frequency increases downward. In this way, the mass increase is always pointed upward in all graphs.

Scanning electron micrographs were taken either on a Model SX-40A ISI (International Scientific Instruments) or on a Super II ISI instrument coupled to a 5500 X-ray spectrometer (Kevex-ray) with a Hitachi monitor for elemental analysis. The electron beam intensity was 20 keV.

X-ray diffractions were obtained using Cu Kα (λ = 1.541 78 Å) irradiation through the Ni filter of an XRD-6 General Electric spectrometer.

Results and Discussion

Pyrrole Electropolymerization. Applying a potential step from $E = 0$ to $E = 650$ mV to an aqueous deoxygenated 2.0×10^{-2} M pyrrole solution in the presence of a 0.10 M NaCl-supporting electrolyte in the EQCM cell resulted in the development of a typical time-dependent current (Figure 1, curve 1). Pyrrole oxidation and electropolymerization began at a potential of 550 mV. In the first step, a pyrrole cation radical ($Py^{\bullet+}$) is expected to form:[25-27] It then reacts with another pyrrole molecule to form a dimer which can be further oxidized to produce trimers, tetramers, and so on. Lower pyrrole oligomers are partially soluble, but with the increasing carbon chain length, the solubility decreases rapidly and the electrode surface becomes the site for the growing polypyrrole film which is believed to be constituted of long chains with the general structure

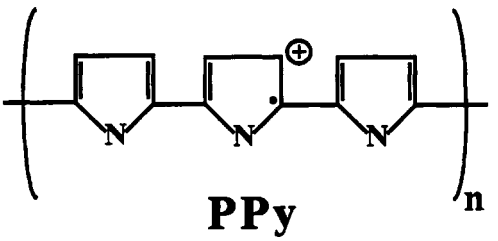

Three-dimensional film growth is likely to result in cross-linked PPy. Electrochemically formed PPy is in its oxidized state and is heavily doped by anions. Thus, it is electronically conducting and can, therefore, continue to grow at the electrode surface. During electropolymerization, the electrode mass increases due to PPy deposition and anionic dopant uptake. This manifests in a decrease in the EQCM oscillation frequency, Δf, as required by eq

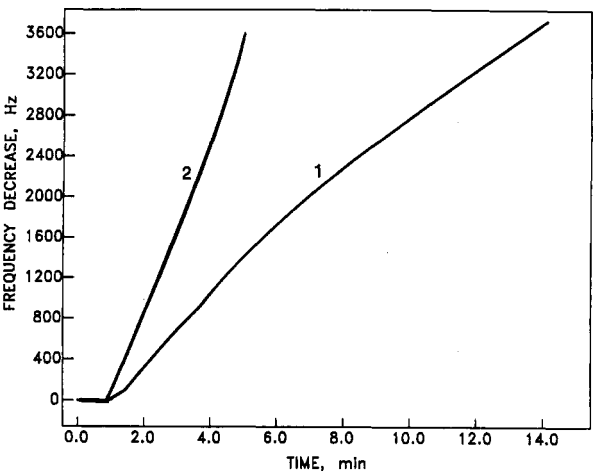

Figure 2. Frequency–time transients obtained at gold modified EQCM electrodes during the polymerization process of an aqueous deoxygenated 2.0×10^{-2} M pyrrole solution containing 0.1 M NaCl in the absence of PSS^- at a potential step of $E = 0$ to $E = 650$ mV (vs SCE; 1) and in the presence of 1.0×10^{-3} M PSS^- at a potential step of $E = 0$ to $E = 600$ mV (2).

1. In the PPy reduction process, excess anions, if mobile, are ejected from the film.[35] This results in an increase in the EQCM oscillation frequency:

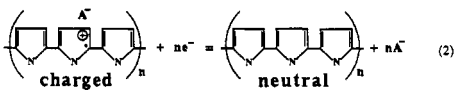

(2)

If the anions are not able to leave (due to their size, steric hindrance, or specific interactions with functional groups of the polymer), then additional cations will enter into the PPy film with a consequent decrease of the EQCM oscillation frequency:[24]

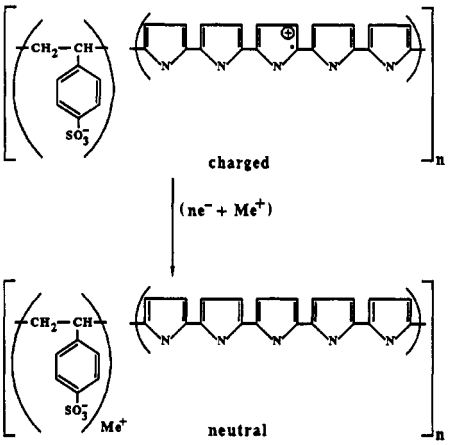

(3)

The total amount of charge passed during electrodeposition of a typical PPy preparation was calculated to be 18.6 mC/cm^2 by numerical integration of the current–time curve. This corresponded to the 77.5-nm thickness of the electrodeposited PPy (assuming 240 mC/μm).[33] Electrooxidation of pyrrole resulted in the electrode mass increase as evidenced by the decrease in the oscillation frequency of the EQCM. The time-dependent changes in Δf are presented in Figure 2, curve 1. The decrease in Δf is compatible with the increase of the mass of PPy de-

(32) Feldman, B. J.; Burgmayer, P.; Murray, R. W. *J. Electrochem. Soc.* **1985**, *107*, 872.
(33) Martin, C. R.; Rubinstein, I.; Bard, A. J. *J. Am. Chem. Soc.* **1982**, *104*, 4817. Wallace, G. G.; Lin, Y. P. *J. Electroanal. Chem.* **1988**, *247*, 145.
(34) Asavapiriyanout, S.; Chandler, G. K.; Gunawardena, G. A.; Pletcher, D. *J. Electroanal. Chem.* **1989**, *177*, 245.
(35) Kaufman, J. H.; Kanazawa, K. K.; Street, G. B. *Phys. Rev. Lett.* **1984**, *53*, 2461.

posited on the substrate, as well as the increase of the uptake of Cl^- ions balancing the charges of the polarons and bipolarons formed during electropolymerization.

PPy/PSS⁻ Electrodeposition. Subjecting an aqueous deoxygenated 2.0×10^{-2} M pyrrole solution to a $E = 0$ to $E = 600$ mV potential step in the presence of 1.0×10^{-3} M PSS^- and 0.1 M NaCl resulted in typical time-dependent current and time-dependent Δf changes (Figure 1, curve 2, and Figure 2, curve 2, respectively). These data are consistent with the formation of PPy/PSS^- composites.[19-24] While the shape of the current transient in the presence of PSS^- was found to be qualitatively similar to that obtained in its absence (Figure 1, curve 1), the magnitude of the pyrrole oxidation current was considerably higher. Integration of the current transient of a typical PPy/PSS^- preparation (Figure 1, curve 2) led to a charge density of 52.0 mC/cm², which was much higher than that observed during the electropolymerization of PPy in the absence of PSS^- (18.6 mC/cm², vide infra). Since pyrrole oligomers are partially water soluble, the increased oxidation current might be the consequence of an efficient electron-transfer reaction followed by a mass transport controlled out-diffusion of the intermediates into the bulk solution. The observed increase in the oxidation current does not necessarily imply a faster rate of electropolymerization for the PSS^- doped polypyrrole. An examination of the Δf vs time plot (Figure 2, curve 2), however, unambiguously demonstrates the increased growth rate of the PPy/PSS^- composite film. Decrease of the oscillation frequency of the quartz crystal is seen to be much faster in the presence of PSS^- at a 0–600 mV potential step (Figure 2, curve 2) than in its absence, even at a higher deposition potential (0–650 mV, Figure 2, curve 1). This behavior may be rationalized by assuming a lowered energy barrier to the PPy growth by electrostatic stabilization of polarons and bipolarons by pyrrole oligomer PSS^- complexes.

Cadmium Ion Uptake by and CdS Formation in PPy/PSS⁻ Composite Films (Method I). Dynamic characteristics of PPY films can be changed by doping them with such a large polyanionic dopant as PSS^-. PPy/PSS^- composite films have predominant cationic dynamics in contrast to their parent PPy films which are predominantly anionic. The reversal of the slope of frequency–potential characteristics in standard electrolyte solutions is indicative of cation uptake occurring during polymer reduction. We observed a change here in the type of ion dynamics, from predominantly anionic to predominantly cationic. Since cations differ in size and the diameters of the channels in the polymeric film may be smaller than those of the penetrant cation, a detailed analysis of the frequency variation upon polymer reduction has to be performed in order to confirm the uptake of Cd^{2+} ions by the composite material in question. Taking the contribution of counterion movement into consideration, potential step experiments can provide a means for such an analysis.

Potentiostatic conditions with E = –600 mV were employed to inject aliquots of Cd^{2+} ions into the electrolyte solution bathing the PPy/PSS^- composite-film-coated electrode. At this potential, no chemical change of Cd^{2+} ions is expected to occur since the potential for Cd^{2+} reduction is –800 mV. An example of the observed mass increase, following the injection of 50 mM Cd^{2+} into the neutral 50 mM NaCl solution bathing the PPy/PSS^- composite-coated electrode, is presented in Figure 3. Changes in the oscillation frequency of the quartz crystal substrate amounted to 3484 Hz (or 3136 ng in terms of

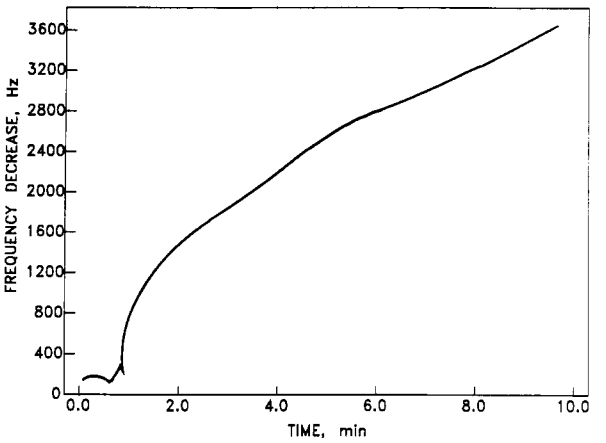

Figure 3. Frequency change–time transients obtained at the PSS^--modified gold EQCM electrode in an aqueous deoxygenated solution containing 5.0×10^{-2} M NaCl following the injection of 5.0×10^{-2} M $CdCl_2$ at a potential of $E = -600$ mV (vs SCE).

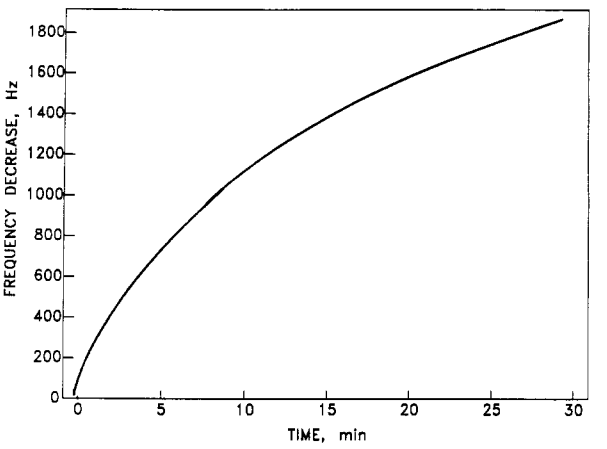

Figure 4. Frequency change–time transients obtained at the Cd^{2+}-incorporated PPy/PSS^--modified gold EQCM electrode in an aqueous deoxygenated solution containing 5.0×10^{-2} M NaCl subsequent to the addition of 5.0×10^{-2} M Na_2S at a constant potential of $E = -600$ mV (vs SCE).

mass units) which corresponded to the exchange of Na^+ ions to Cd^{2+}. However, the magnitude of this effect was far beyond the electrostatic balance requirement, even if all of the Na^+ ions had been exchanged to Cd^{2+} ions. Attraction of additional Cd^{2+} ions to the functional groups of PPy/PSS^- had to be assumed, most likely in the form of ion pairs. The dielectric properties at the surface of thin films are known to be different from that in the bulk. The environment of the composite polymer may actually destabilize the hydration shell of ions and cause a considerable shift toward the increased formation of ion pairs. Regardless of the mechanism of cadmium incorporation, the experimental finding of large quartz frequency changes are attributable to the mass increase due to the uptake of large amounts of Cd^{2+} ions into the composite polymer film.

Subsequent to exchanging Cd^{2+} by Na^+, the solution bathing the PPy/PSS^- films was adjusted to contain 5.0×10^{-2} M HS^- by injection of appropriate amounts of Na_2S. Frequency changes were then monitored as a function of time. The obtained frequency–time transient of a typical preparation is presented in Figure 4. The total decrease of the quartz frequency was 1871 Hz, which corresponded to a mass increase of 1684 ng. The experiment was carried out at constant potential $E = -600$ mV. No evidence was obtained for the formation of elemental sulfur under these conditions. The entire mass increase can be associated

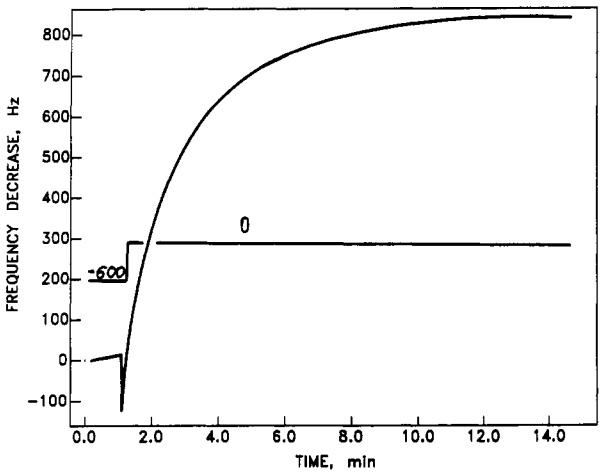

Figure 5. Frequency change–time transients obtained at the PPy-modified gold EQCM electrode in an aqueous deoxygenated solution containing 5.0×10^{-2} M Na_2S at a potential step of E = –600 to E = 0 mV (vs SCE).

with the uptake of HS^- ions into the PPy/PSS^- films (and associated counterion movement) and their subsequent reaction with Cd^{2+} ions held in the film.

Insertion of Elemental S and CdS Formation in PPy Films (Method II). Elemental sulfur can be inserted into the polypyrrole matrix from a bisulfide solution when the film has predominantly anionic dynamics by selecting the operating potential in the oxidation region of the polymer. Bisulfide ions, attracted to polarons and bipolarons, are oxidized and immobilized as elemental sulfur at the appropriate anodic potential within and at the surface of the PPy film. In the pH region 7.0–13.9, HS^- predominates and the electrode reaction and the corresponding Nernst equations are given as

$$S + H^+ + 2e^- = HS^-$$
$$E_{eq} = E^\circ - 29.58\ pH - 29.58 \log(a_{HS^-}) \quad (4)$$

with E° = –65 mV (vs NHE). At a pH of 10.0 and HS^- activity of 5×10^{-2} M, the equilibrium potential of the sulfur/bisulfide ion electrode is E_{eq} = –563 mV vs SCE. Using EQCM, sulfur was found to form at PPy-coated gold electrodes at potentials of E > –500 mV vs SCE. Note that both the concentration of HS^- and ionic strength in the PPy film are different from those in bulk solution.

Applying an E = –600 mV to E = 0 mV potential step to the aqueous 50 mM HS^- solution bathing the PPy film in the EQCM cell resulted in typical time-dependent Δf changes as shown in Figure 5. The decrease in the oscillation frequency of the quartz crystal substrate, amounting to 843 Hz, was indicative of the uptake of 759 ng of sulfur species (both the bisulfide ion and the elemental sulfur) into the film. This mass increase is larger than that observed during the insertion of Cl^- ions upon PPy oxidation in the absence of HS^- in similar potential step experiments. The mass increase due to the Cl^- ion uptake was 300 ng.

PPy films with immobilized elemental sulfur were then subjected to ion exchange by immersion into a 0.1 M NaCl solution. In this operation, sulfide species in the film were replaced by chloride ions. Washing and ion exchange were necessary to avoid clogging of the PPy surface by excess colloidal CdS. No frequency change was observed when the potential was kept at E = 0 mV (i.e., at the level of sulfur insertion) upon the addition of 0.1 M NaCl and 50 mM Cd^{2+}. Apparently, the attraction of Cd^{2+} ions requires excess negative charge at the PPy film. This was accomplished by the ejection of polarons and bipolarons and by

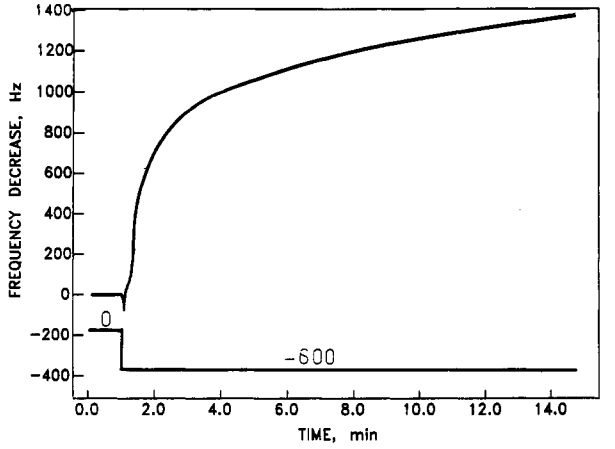

Figure 6. Frequency change–time transients obtained at a PPy/S^0-modified gold EQCM electrode in an aqueous deoxygenated solution of 5.0×10^{-2} M $CdCl_2$ containing 0.1 M NaCl at a potential step of E = 0 to E = –600 mV (vs SCE).

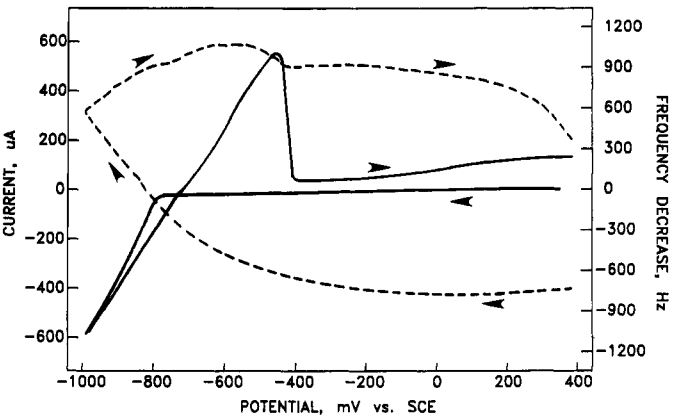

Figure 7. Linear potential scan of the current (solid line) and of the frequency (dashed line) vs potential at a PPy/CdS-modified gold EQCM electrode in an aqueous deoxygenated 5.0×10^{-2} M $CdCl_2$ solution. A triangular waveform was used with a scan rate of 50 mV/s in the potential range of E = +400 to E = –1000 mV (vs SCE).

the reduction of immobilized elemental sulfur. The sulfidic sulfur formed during the reduction process also provided additional negative charges which increased the film's ability to attract Cd^{2+} ions from the solution.

Frequency changes of a typical PPy Au piezoelectrode, bathed in an aqueous 0.1 M NaCl + 50 mM Cd^{2+} solution, upon the application of a potential step from E = 0 to E = –600 mV are illustrated in Figure 6. The decrease in the oscillation frequency of the quartz crystal substrate amounted to 1373 Hz, which corresponded to a 1236-ng mass increase. This mass increase was due to the uptake of Cd^{2+} ions into the PPy film. The Cd^{2+} ions entered the film, neutralized the exposed HS^- ions, and initiated CdS nucleation and subsequent growth.

Potentiodynamic characteristics play an important part in the development of the procedures for CdS incorporation into PPy films. Special care had to be taken in choosing the potential (–600 mV; Figure 7) in order to avoid the electroreduction of Cd^{2+} ions entering the polymer film and the formation of crystallites of metallic cadmium. The thermodynamic equilibrium potential for a cadmium metal–cadmium ion electrode in a 5×10^{-2} M solution of cadmium ions is E_{eq} = –682 mV vs SCE (assuming E° = –403 mV vs NHE). The small difference between the observed current onset potential and the theoretical E_{eq} may be due to different concentrations of Cd^{2+} ions in the film and in the bulk solution, to the effect

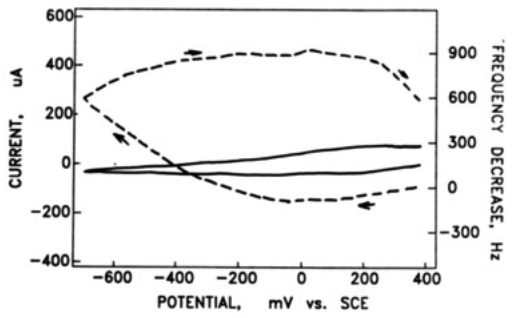

Figure 8. Linear potential scan of the current (solid line) and of the frequency (dashed line) vs potential at a PPy/CdS-modified gold EQCM electrode in an aqueous deoxygenated 5.0×10^{-2} M $CdCl_2$ solution. A triangular waveform was used with a scan rate of 50 mV/s in the potential range of $E = +400$ to $E = -600$ mV (vs SCE).

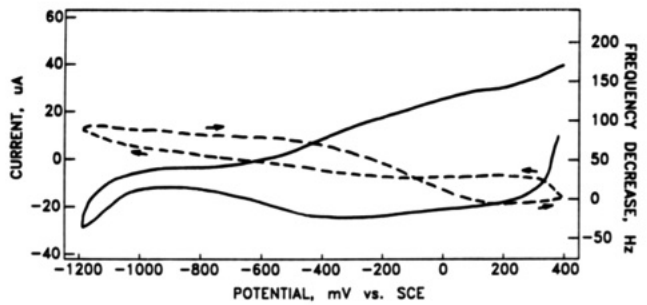

Figure 9. Linear potential scan of the current (solid line) and of the frequency (dashed line) vs potential at a 0.077-μm-thick PPy modified gold EQCM electrode in an aqueous deoxygenated 0.1 NaCl solution in the presence of CdS particles. Scan rate: 50 mV/SCE (vs SCE).

of ionic strength in the film and in solution, and to kinetic retardation of cadmium deposition. The difference in solvation energy of Cd^{2+} ion in the bulk solution and in the film may also be a factor. Upon scan reversal, the metallic cadmium formed began to dissolve at approximately the same potential and a wide anodic stripping peak appeared in the voltammetric curve (Figure 7). Mass changes did not follow the electrochemical processes exactly. It is likely that metallic cadmium deposited inside the PPy film or at the PPy–Au interface, rather than at the PPy film–aqueous solution interface. Thus, oxidation of metallic cadmium did not cause any immediate mass decrease since the Cd^{2+} ions formed required finite time to diffuse through the polymer film. Initiation of the oxidation of metallic cadmium (reflected by the raising branch of the anodic stripping peak) did not result in an immediate frequency increase, i.e. mass decrease (Figure 7). This observation supports the postulated assumption of cadmium deposition at the PPy–Au interface. Since the oxidation of Cd^0 from the film would cause a considerable charge imbalance in the absence of any release of Cd^{2+}, we must assume that some charge balancing processes take place here. One possibility is that anions enter the film from the solution and cations (Na^+) are ejected from the film. However, the small mass variation indicates that an extensive water dissociation may take place in the film. The hydrogen ions produced are being ejected from the film to satisfy the charge balance. Very strong pH variation in PPy films has recently been reported.[36]

Linear potential scan characteristics of the PPy/CdS films showed considerable differences in ion dynamics compared to the films examined prior to CdS incorporation. The voltamperometric and microelectrogravimetric characteristics are presented in Figure 8. The voltammogram (solid line) did not indicate any new features that could be ascribed to the electrochemical decomposition of CdS. The frequency–potential curve showed preferential cation dynamics and a large hysteresis in the electrode mass variation upon potential scanning, which is likely to

(36) Shinohara, H.; Kojima, J.; Aizawa, M. *J. Electroanal. Chem.* **1989**, *266*, 297.

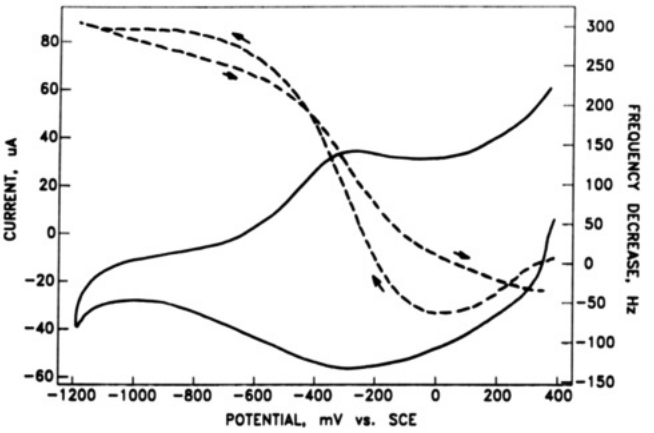

Figure 10. Linear potential scan of the current (solid line) and of the frequency (dashed line) vs potential at a PPy/CdS-modified gold EQCM electrode in an aqueous deoxygenated 0.1 M NaCl solution. The PPy film thickness was assessed to be 0.232 μm.

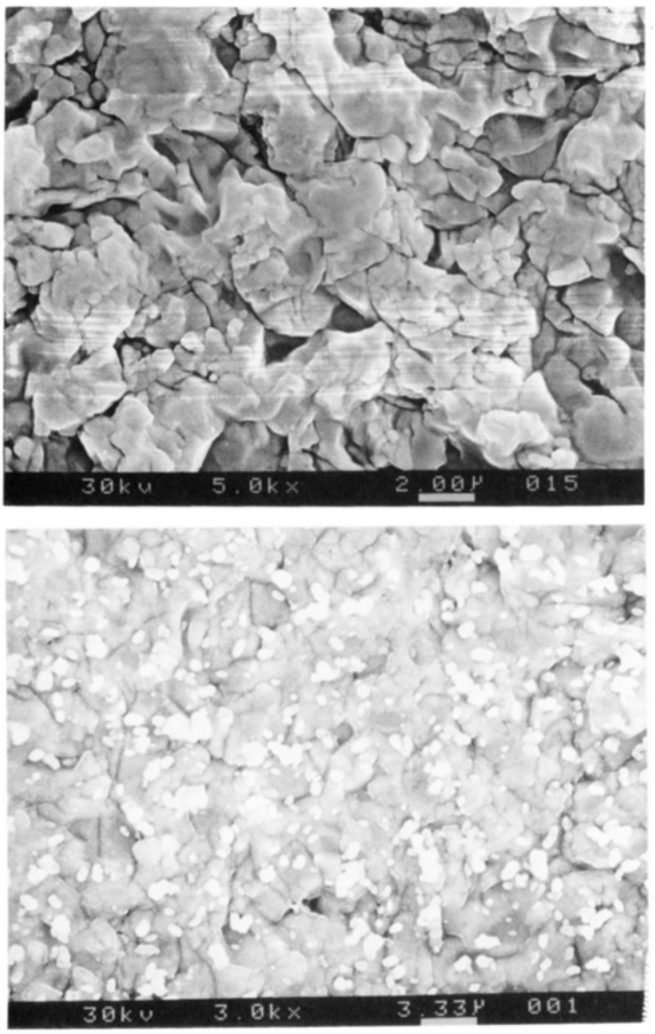

Figure 11. Scanning electron micrographs of a PPy film (prepared by method I) on a gold-coated quartz substrate in the absence (top photograph) and in the presence (bottom photograph) of CdS particles.

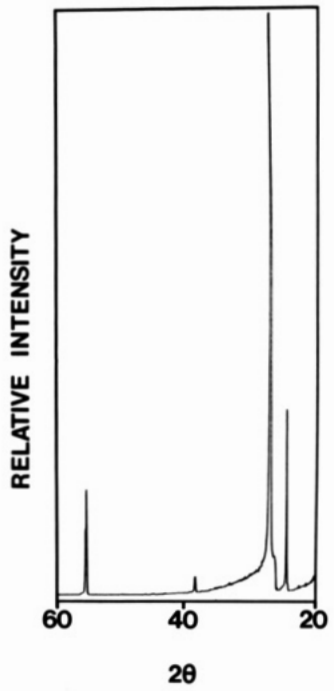

Figure 12. Intensities of X-ray diffraction against the angles between the incident and scattered direction (2θ) for a CdS-containing PPy film (prepared by method II) on a gold-coated quartz substrate.

be related to the larger ionic size of Cd^{2+} than that of Na^{+}.

Properties of the PPy film change considerably after the incorporation of CdS particles. The voltamperometric and microelectrogravimetric characteristics of a thin CdS-particle-containing PPy film in 0.1 M NaCl are presented in Figure 9. The potential dependence of the oscillation frequency (dashed line) showed preferential cation dynamics. The corresponding maximum mass changes were within the range of 100 ng for thin films (0.077 μm). For films 3 times thicker, mass changes were found to increase by a factor of 3. Thicker films were found to be able to accommodate more Cd^{2+} ions. The current–potential characteristics (Figures 9 and 10, solid lines) for PPy/PSS^{-}/CdS films showed good reversibility, indicating the electroinactivity of CdS in the potential range investigated. Contribution of weakly conducting particles to the total conductance is related, of course, to their volume fraction.

Characterization of Electrogenerated CdS Particles in PPy and PPy/PSS^{-} Films. The morphology of polypyrrole films has been examined by scanning electron microscopy (SEM). SEM micrograms indicated the presence of irregular CdS particles in the 80–150-nm range (Figure 11). X-ray diffractometry was used to establish the chemical composition of these particles. Intensities of X-ray diffraction appeared at 2θ angles (2θ = the angle between the incident and scattered direction of the X-ray) of 54.6°, 44.4° (only seen upon enlargement of the vertical scale), 38.3°, 28.0°, 26.4°, and 24.9° (Figure 12). Angles at 24.9°, 26.4°, 28.0°, and 54.6° are in the range associated with microcrystalline CdS.[36] Furthermore, in the absence of CdS, the only angles which appeared in an identical PPy film (taken also on a gold-coated quartz substrate) were at 38.3° and 44.4°, and a broad maxima centered at 28.0°. Angles of 38.3° and 44.4° were attributed, therefore, to gold in accordance with the tabulated values.[37] Cadmium also has a characteristic X-ray diffraction angle at 38.3°,[37] thus,

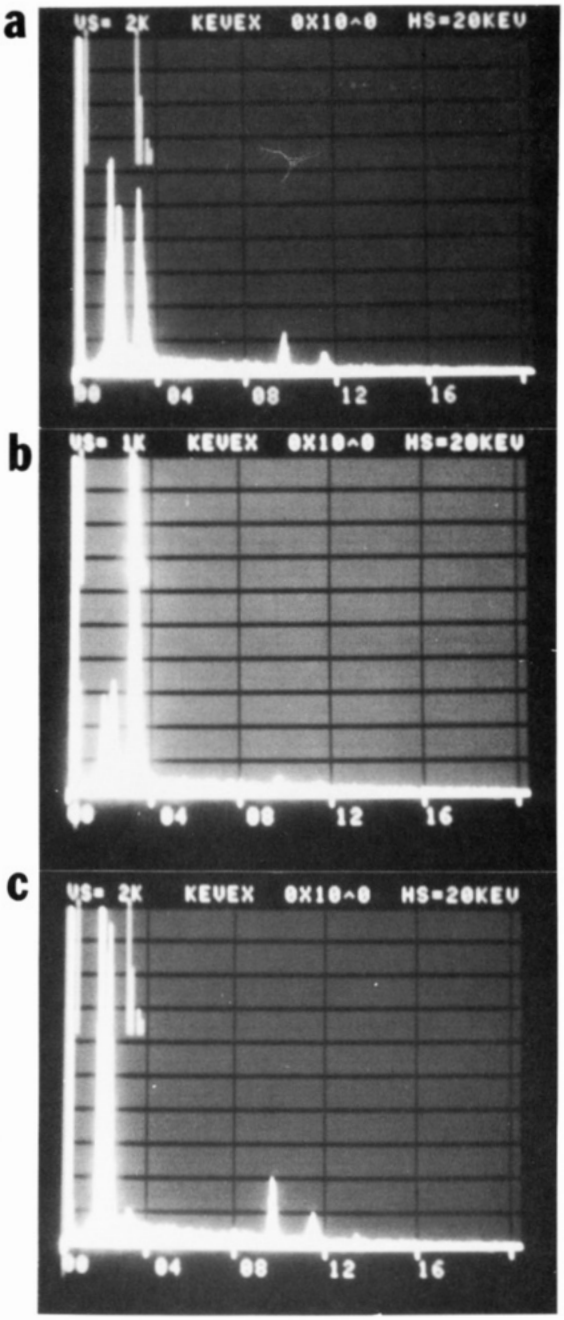

Figure 13. Intensities of X-ray as functions of X-ray energy taken at different parts (a–c) of the same sample of CdS-containing PPy film on a gold-coated quartz substrate.

the possibility of having some cadmium in the samples cannot be excluded. The broad X-ray diffraction band, centered around 28.0°, was similar to that observed in the quartz substrate reference and it was ascribed, therefore, to it. Poorly crystalline PPy showed, as expected,[38] a completely structureless diffraction pattern with no maxima.

Intensities of X-ray as functions of X-ray energy, taken at three different parts of the same CdS-containing PPy film (on a gold-coated quartz crystal substrate), are shown in Figure 13. Intensities at 1.75, 2.30, and 3.14 keV correspond to Si (K_α), S (K_α), and Cd (L_α), while those at 9.68 and 11.44 keV are due to Au (L_α, L_{III}, respectively). Intensities of Cd to S appear to vary from spot to spot, indicating a high degree of nonuniformity in the electro-

(37) Powder Diffraction File, Published by the Joint Committee on Powder Diffraction Standards, 1845 Walnut Street, Philadelphia, PA 19103; 1960, 1967, 1971.

(38) Geiss, R. H.; Street, G. B.; Volksen, W.; Economy, J. *IBM J. Res. Dev.* **1983**, *27*, 321.

chemically generated CdS particles.

Conclusion

The most significant accomplishment of the present work has been the demonstration of electrochemical generation of CdS particles in the matrices of conducting polymers. Advantage has been taken of ion incorporation dynamics under potential control to introduce the necessary precursors into the polymer matrices. Thus, Cd^{2+}, incorporated into negatively charged PPy/PSS^- polymer composites, has been converted to CdS by the subsequent introduction by HS^- ions. Alternatively, HS^- ions, introduced into positively charged PPy, provided a useful precursor for attracting Cd^{2+} and for the subsequent CdS formation. The EQCM has played a pivotal part in the optimization of the required experimental conditions. Although at present we could only produce irregular CdS particles, we are confident that judicious improvements of the experimental methodology will allow the formation of size-controlled and dimensionally reduced semiconductor particles in the matrices of conducting polymers.

Acknowledgment. Support of this work by a grant from the Department of Energy is gratefully acknowledged. M.H. thanks the National Science Foundation for a Research Opportunity Award. D.Y. is the holder of a Chaim Weizmann Postdoctoral Fellowship for Scientific Research.

Registry No. PSS^-Na^+, 9080-79-9; CdS, 1306-23-6; Cd, 7440-43-9; pyrrole (homopolymer), 30604-81-0.

Crystallization Behavior of Xerogels in a Cr_2O_3-Doped SiO_2–Al_2O_3–ZnO System

W. Nie and G. Boulon*

Laboratory of Physical Chemistry and Luminescent Materials, University Claude Bernard Lyon I, UA CNRS 442, 69622 Villeurbanne, France

C. Mai and C. Esnouf

GEMPPM, INSA of Lyon, UA CNRS 341, 69621 Villeurbanne, France

Xu Runjuan and J. Zarzycki

Laboratory of Sciences of Vitreous Materials, UA 1119, University of Montpellier 2, 34060 Montpellier Cedex 1, France

Received May 9, 1991. Revised Manuscript Received November 12, 1991

Nucleation, crystallization, and characterization of nanocrystallites and xerogels of the Cr_2O_3-doped SiO_2–Al_2O_3–ZnO system have been studied. The techniques used are X-ray diffraction, small-angle X-ray scattering, transmission electron microscopy, optical absorption, and laser spectroscopy techniques.

Introduction

In previous papers we have explained our approach to research on nucleation induced in gahnitelike glasses or xerogels by chromium oxide.[1-3] Indeed, the chromium element is both an excellent nucleating agent and a good structural fluorescent probe so that we may apply to such systems scattering techniques and laser spectroscopy, which are complementary techniques in the characterization of materials. The first part of our program dealt with glasses of SiO_2–Al_2O_3–MgO and SiO_2–Al_2O_3–ZnO[2] systems. In the present work we will present new data on the SiO_2–Al_2O_3–ZnO system synthesized by the sol–gel route, keeping the same initial compositions as that of glasses synthesized by the standard method. Under different heat treatments from 50 to 1000 °C, we follow the transitions sol–gel → glass → glass–ceramic. In addition to understanding the nucleation mechanism, another motivation is to improve our knowledge on the optical properties of gels. To this end, several xerogel samples were prepared with various proportions of components and were analyzed by X-ray diffraction, small angle X-ray scattering (SAXS), transmission electron microscopy (TEM), energy dispersive X-ray spectroscopy, optical absorption, and laser spectroscopy techniques. We will give the main structural results in the continuous transformation of the samples under thermal treatment from low to high temperature.

Experimental Section

The preparation of xerogels and characterization methods are described in ref 3. SAXS measurements were carried out using a special camera mounted on a Rigaju rotating anode (12 kW) X-ray generator. A one-dimension position-sensitive detector and a multichannel analysis system connected to a microcomputer allowed rapid measurements. A pointlike slit conditions with an irradiated cross section of about 1 mm^2 was used. This type of collimation avoided mathematical desmearing. This is essential to improve the accuracy of the experimental results in order to study the fractal behavior. Both the sameple and the X-ray beam of wavelength 1.54 Å were in vacuum to reduce air scattering. Scattering curves were obtained in the range of vector $\mathbf{q} = (4\pi \sin \vartheta/\lambda)$ from 10^{-2} to 5×10^{-1} $Å^{-1}$. The parasitic scattering from holder and slits was subtracted from the experimental SAXS intensity.

TEM observations were performed on a 200 CX Jeol microscope. Thin samples were prepared by a crushing technique. The glass powder was deposited on carbon film from a suspension of

(1) Ponçon, V.; Bouderbala, M.; Boulon, G.; Lejus, A. M.; Reisfeld, R.; Buch, A.; Ish-Shalom, M. *Chem. Phys. Lett.* **1986**, *130*, 444.
(2) Ponçon, V.; Nie, W.; Boulon, G. *Eur. J. Solid State Inorg. Chem.* **1989**, *26*, 53-70.
(3) Nie, W.; Boulon, G.; Maï, C.; Esnouf, C.; Rundjuan, Xu; Zarzycki, J. *J. Non-Cryst. Solids* **1990**, *121*, 282-287.

0897-4756/92/2804-0216$03.00/0